

# Electrodynamic Shaker Fundamentals

George Fox Lang, Data Physics Corporation, San Jose, California

The electrodynamic shaker is a commonplace tool for most readers of this magazine. Yet, many of us have never taken the time to really understand the subtle mechanisms at play in the operation of this workhorse. This article attempts to rectify this oversight by presenting some basic experimental observations from several viewpoints.

The electrodynamic shaker functions to deliver a force proportional to the current applied to its voice coil (see sidebar). These devices are used in such diverse activities as product evaluation, stress screening, squeak-and-rattle testing and modal analysis. These shakers may be driven by sinusoidal, random or transient signals based upon the application. They are invariably driven by an audio-frequency power amplifier and may be used "open loop" (as in most modal testing) or under closed-loop control where the input to the driving amplifier is servo-controlled to achieve a desired motion level in the article under test.

## Pluck It!

A surprising amount of information may be extracted from a shaker by using it as a vibration sensor, rather than as an exciter. In such an experiment, the voltage output of the voice coil is monitored while the shaker is caused to vibrate due to transient mechanical input. Measuring the dynamic response of the shaker with its table bare and, again, with a known mass attached to the load table permits the suspension characteristics to be determined. Figure 1 shows a typical small permanent magnet shaker and the apparatus used in such a test.

Figure 2 illustrates a "pluck" test. The shaker is forced against its lower stroke-stop and held under pressure. This is abruptly released to allow the shaker to "ring." On a small shaker such as this one, the human fingernail is an ideal load/release tool; larger units may require alternate transient load-release fixturing. The coil voltage should be monitored with an instrument of high input-impedance, capable of FFT analysis.

Figure 3 shows the time histories resulting from a "pluck" with the table bare and with an attached mass-load. In this instance, the differentiating load is a 23.61 gram (0.8311 oz/g) accelerometer. The response of the shaker has a classic single degree-of-freedom form – it rings down sinusoidally with an exponential envelope. Note that attaching a mass reduces the frequency of the ring-down and decreases the rapidity of exponential collapse; both effects are anticipated from a simple spring-mass-damper model.

Figure 4 shows the spectra of the unburdened and mass-loaded ring-downs. The frequency at peak response indicates the natural frequency of the shaker's suspension system (without bias) as the measured voltage is proportional to the table and voice-coil velocity. Cursor measurements from Figure 4 disclose a resonant frequency  $f_n$  of 48.4375 Hz for the unloaded shaker and a mass-loaded frequency  $f_a$  of 36.7188 Hz with the additional mass  $M_a$  attached. The half-power (-3 dB) points bounding  $f_n$  in the stud-only condition were found to be separated in frequency by  $\Delta f_{3dB} = 34.8438$  Hz.

These observations permit evaluating the mass, stiffness and damping of the shaker suspension in accordance with the following equations (presented without derivation). Specifically, the effective mass  $M$  of the shaker in unburdened configuration was found to be 31.27 grams (0.03127 kg) or  $178.4 \times 10^{-6}$  lb sec<sup>2</sup>/in. (1.103 oz/g) from Equation (1). The suspension stiffness  $K$  was evaluated from Equation (2) as  $2.896 \times 10^6$  dyne/cm ( $2.896 \times 10^3$  N/m) or 16.54 lb/in. The viscous damping rate  $C$  was found to be  $6.846 \times 10^3$  dyne sec/cm (6.846 Ns/m) or  $39.09 \times 10^{-3}$  lb sec/in. from Equation (3).



Figure 1. Two small electrodynamic shakers illustrate the mass loading used in "pluck" tests. The unit on the left has an (essentially) bare table; only a 0.72 gram beryllium-copper 10-32 UNF mounting stud is installed. A 23.61 gram accelerometer is fitted to the unit on the right.



Figure 2. "Pluck" testing a shaker. The finger depresses the table against its limit stop, then releases it abruptly. The transient voltage generated by the shaker coil is measured with a high impedance instrument.

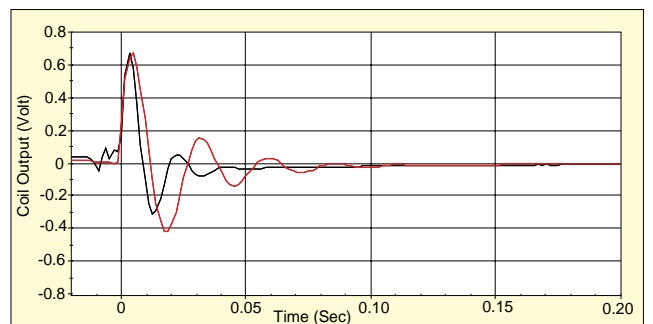


Figure 3. Time-histories of shaker coil voltage generated by "plucking" the shaker exhibit classic single degree-of-freedom, damped exponential form. Both configurations of Figure 2 are shown; note that adding mass (red) reduced the natural frequency and the damping, as expected.

$$M = M_a f_a^2 / (f_n^2 - f_a^2) \quad (1)$$

$$K = (2\pi f_n)^2 M \quad (2)$$

$$C = 2\pi \Delta f_{3dB} M \quad (3)$$

## A Damped Surprise

Initial experiments with the shaker showed an astonishing difference in response between a bare table and one in which a 10-32 mounting stud was installed. For this reason, the prior comparisons were made with a mounting stud installed in both instances. This seemed reasonable as a stud or screw is required

## Setting a Shaky Foundation

There are many types of machines designed to deliberately vibrate structures. Several photographs in this article show small, permanent magnet, electrodynamic shakers. These are very popular drivers in the under 100 lbF range. Larger electrodynamic shakers frequently employ dc-excited electromagnets, but their operating principles are very similar to the permanent magnet unit discussed here. Electrodynamic shakers are relatively inexpensive, easy to control, simple to interface and quite linear in their behavior (if used within their specified force and motion limits).

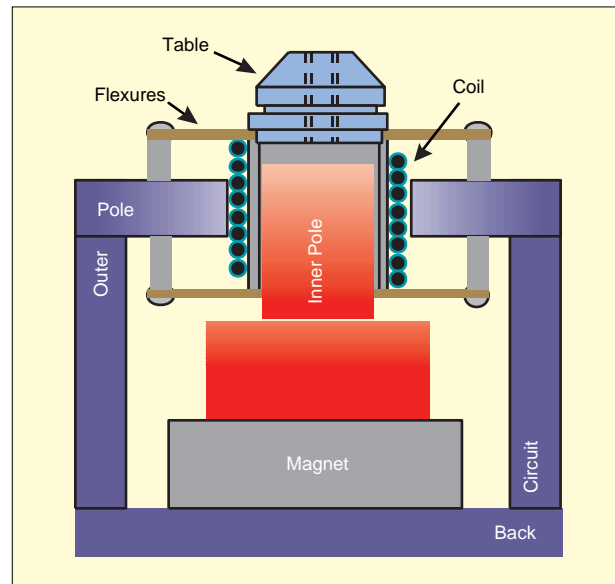
The structure of these machines bears some resemblance to a common loud-speaker but is heavier and far more robust. The schematic figure, above, is provided to spare you violating the warrantee of a prized tool! It shows a sectioned-view of the shaker with emphasis on the magnetic circuit and suspended driving table.

At the heart of the shaker is a single-layer coil of wire, suspended in a radial magnetic field. When a current is passed through this coil, a longitudinal force is produced in proportion to the current and this is transmitted to a table structure to which the test article may be affixed. Several items of design detail are worthy of examination.

Firstly, some ingenuity is required to produce the radial magnetic field acting in a plane normal to the coil's axis. This is accomplished by building a magnetic circuit of permeable iron or steel around an axially polarized cylindrical magnet. As shown, an inner pole piece transmits flux from one end of the magnet, say the north face. A permeable disk conducts flux to the opposite, say south polarized, surface of the magnet. In turn, this disk is intimately connected to a permeable cylindrical tube which mates to another permeable disk with a hole in its center surrounding the coil. This second disk is the outer pole piece. Thus the inner pole is north-polarized and surrounded by a torus which is south-polarized. This results in a radial flux field through the gap between these ferrous parts.

Secondly, the coil must be allowed to move axially but be restrained from all other motions. It must be accurately centered in the narrow gap between the inner and outer poles. The coil is wound around the outer diameter of a stiff thin-walled tube, the coil form. The drive table is rigidly attached to one end of the coil form. Each end of the coil form is also affixed to a compliant (slotted) disk or to sets of radial beams. These are the support flexures which hold the coil form concentric between the pole pieces and restrain any out-of-plane moments applied to the drive table. The flexures are secured to the outer pole piece via spacers and screws or rivets. Flexible conductors attach to the ends of the coil and connect them with the input connector on the body of the shaker.

Thirdly, the force provided by the machine is proportional to the magnetic flux passing through the coil, to the current flowing through the coil and to the number of coil-turns within the flux. For this reason, the coil is normally longer than the width of the outer pole by at least the intended stroke of the machine. In general, shaker coils use heavier conductors than speakers so that they may accommodate heavier currents. Hence, shaker coil resistance will be lower than that of common speakers, a factor to bear in mind when selecting a companion drive-amplifier. The air-gap between the pole pieces wants to be minimized to reduce the reluctance



tance of the magnetic circuit and thus maximize the intensity of the magnetic field. The thickness of the outer pole piece is optimized when that element is just barely saturated; the same constraint applies to the entirety of the back circuit formed by (at least) three mated metallic parts. There is a certain amount of "arcane art" in designing efficient magnetic circuits as the exact field shapes and conveyed flux densities are difficult to predict. Most available shakers are old designs refined over the years by mechanical "cut-and-try" methodology.

Fourthly, the coil impedance is complex. The coil couples strongly with the iron of the pole pieces, yielding a significant inductive component in its impedance. The coil (dc) resistance defines the *minimum* impedance exhibited at the shaker input terminals; the (ac) impedance increases directly with frequency, owing to this term.

Finally, the interplay between the electrical and mechanical domains is not a "one-way street". When the coil moves within the magnetic field, a voltage is generated across the coil in proportion to the velocity experienced by the suspended components. This "back emf" is seen in the electrical domain as an increase of the shaker's coil impedance and reflects the mechanical activity into the electrical circuit.

Back emf can also be generated in conductive coil forms (when used). Since such a coil form constitutes a single-turn "short circuit", it dissipates energy in resistive heat. This reflects itself in the mechanical system as a damping force. The drive coil itself is also a damping mechanism; the extent of its effectiveness in this role is determined by its resistance and by the output impedance of the amplifier which drives it. Other damping mechanism are present in the machine including hysteresis of the flexures and "windage" within the shaker.

The prudent shaker operator uses his machine well within its design envelope. This implies use within the specified maximum table acceleration, velocity and stroke limits, delivery of no more than the rated maximum force, consumption of rms current less than the continuous duty rating and avoidance of load eccentricity beyond the rated moment restraint of the machine.

to mount anything to the shaker's table. Additional investigations were undertaken to understand this observation.

As shown in Figure 5, the shaker was pluck-tested with the mounting hole open and with this small orifice blocked with light plastic tape. Figure 6 shows the resulting time histories, while Figure 7 presents the corresponding spectra. It is evident

from these measurements that blocking this port has a profound effect on the evidenced damping and only a slight effect on the apparent stiffness. With the mounting hole open the shaker exhibited a natural frequency of 53.4375 Hz and a 3 dB bandwidth of only 5.46875 Hz.

Blocking the mounting hole with tape or a threaded mount-

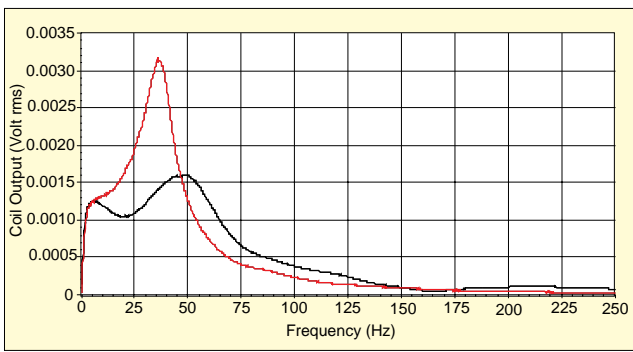


Figure 4. Spectra from the pluck tests shown in Figure 3. Here, the decrease in frequency and the increase in 'Q' due to a mass addition (red) is obvious. The shaker stiffness and moving mass can be determined from the frequency shift, the damping from the exhibited 3 dB bandwidth.



Figure 5. An unanticipated discovery; this shaker's damping is predominated by internal aerodynamic effects. The "pluck" test was conducted on a shaker with an open mounting hole (no stud) and on a unit with the hole blocked by plastic tape.

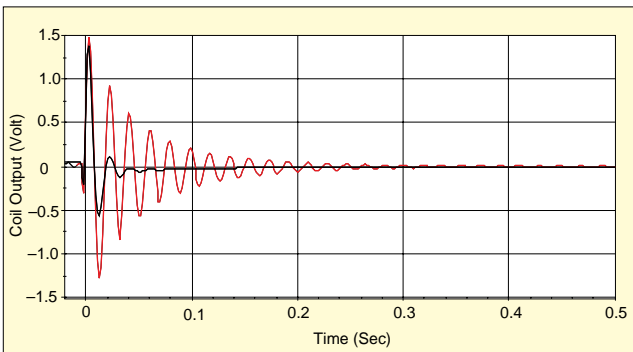


Figure 6. Comparison of transient "pluck" responses with the shaker mounting hole open (red) and blocked by tape (black) as shown in Figure 5. Note the profound difference in damping.

ing stud prevents air from freely moving through it. This clearly means the air within the shaker is forced to expand and compress as the table and coil move. That is, a parallel suspension air-spring is formed. The rate of this spring is inconsequential with regard to that of the flexures. Blocking the port possibly introduces damping because the action of the air-spring is not adiabatic; heat energy may be lost with each compression/expansion cycle. It is also possible that forcing the contained air to shuttle past the moving voice coil simply induces "windage" or drag loss. In any case, from Equation (3) we determine that almost 85% of the previously identified damping rate is attributable to internal aerodynamic effects.

### Reflections in an Electrical Eye

The electrical impedance of the shaker coil reflects the mechanical motion of the shaker table. Clearly, the coil has a re-

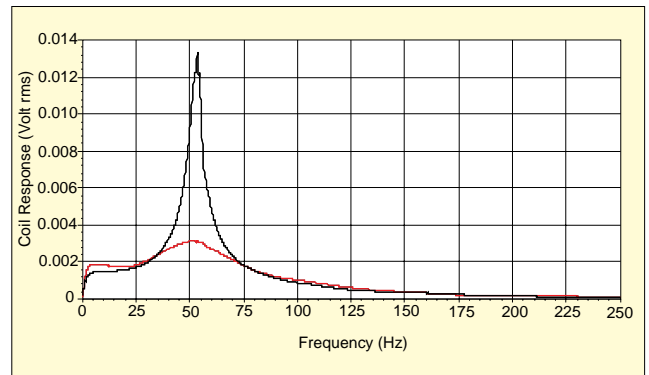


Figure 7. Spectra corresponding to the time histories of Figure 6. Blocking the airflow slightly (red) increases the effective spring rate as might be expected; it dramatically increases the damping which surprised this observer.

sistance  $R$  (typically very low) that may be measured with an ohmmeter (our test specimen exhibited  $1.6 \Omega$  when so measured). As it is a coil, it will also exhibit a series inductance  $L$  which tends to increase the impedance in direct proportion to frequency. But, there is a third element at play. When the coil moves in the magnetic field, a voltage is generated in proportion to the velocity of motion. Thus the voltage  $E$  across the coil may be written in terms of the flowing current  $i$  and the velocity  $V$ :

$$E = R_i + L di/dt + k_1 V \quad (4)$$

Or, restated in the frequency domain:

$$E = (R + j2\pi fL)i + k_1 V \quad (5)$$

The mechanical mobility (velocity/force) of the shaker mechanical components may be represented by a driving-point frequency response function  $H_{fv}$  so that we may state:

$$V = H_{fv} F \quad (6)$$

The coil produces an axial force, acting on the shaker mechanical elements, in proportion to the applied current:

$$F = k_2 i \quad (7)$$

Combining equations (5), (6) and (7) allows us to state the impedance  $Z$  exhibited by the voice-coil:

$$Z = E/i = R + j2\pi fL + k_1 k_2 H_{fv} \quad (8)$$

Thus the *minimum* coil impedance is determined by the (dc) resistance, which is real-valued. The coil inductance contributes an imaginary ( $90^\circ$  phase-shifted) ac component that increases in direct proportion to frequency. The mechanical mobility contributes frequency-dependent terms that exhibit a real maximum at each mechanical resonance. These can significantly *increase* the impedance in a narrow frequency band.

Shaker manufacturers frequently document their products by measuring the coil impedance in two specific circumstances, termed "bare table" and "blocked armature." Figure 8 shows the mechanical arrangement used to conduct these characterizations on our test specimen.

Impedance measurements were obtained by exciting the shaker coil with random noise applied to a small power amplifier. The current was measured with a clamp-on current transformer (see Figure 11) and the voltage at the amplifier's output was measured using an audio-frequency isolation transformer. The low frequency response of the power amplifier limited the ability to apply significant input below about 10 Hz.

Figure 9 compares the impedance measured in these two extreme circumstances. The blocked test basically measures the electrical properties of the coil as though it were simply a wound inductor; this measurement reflects the coupling of the magnetic circuit elements upon the coil. With the exception of some experimental anomalies in the poorly excited region, this trace reflects a near-constant real value at low frequency and a gradual rise in magnitude and phase shift with increas-



Figure 8. Mechanical configurations for traditional coil impedance tests. The unit on the left is unrestrained; the shaker on the right has its table motion “blocked” by a bracket.

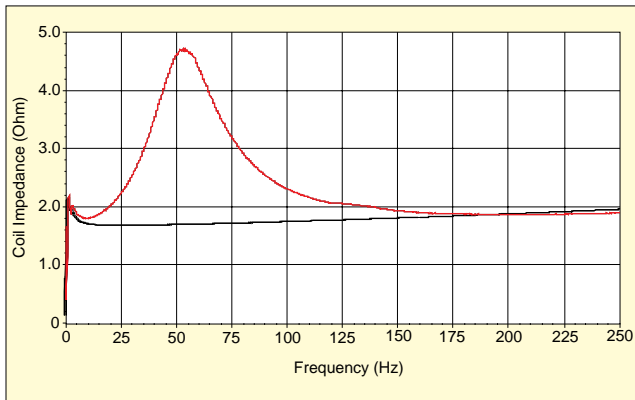


Figure 9. Shaker coil impedance measured with the table blocked (black) and free (red). Note the “reflection” of free-table mobility as a local increase in the electrical impedance. A proportional increase in impedance with frequency can be seen in both traces. In this Figure, a mounting stud is installed in the table.

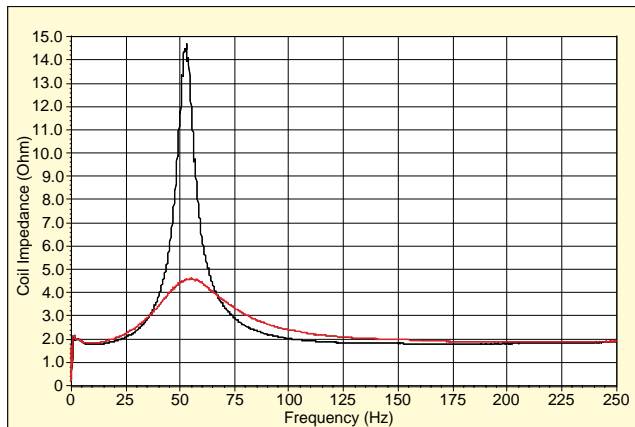


Figure 10. Comparison of shaker coil impedance with the mounting hole open (black) and blocked by tape (red). Note the dramatic increase in impedance that occurs when the suspension damping is minimized.

ing frequency. The bare table impedance shows the addition of an image of the mechanical mobility, reaching a maximum (real) value at the resonant frequency of the unburdened suspension system. These results are consistent with Equation (8).

The “bare table” measurement of Figure 9 was actually made with a 10-32 mounting stud in the mounting hole for the reasons previously discussed. Figure 10 investigates the influence of the damping imposed by blocking this hole. In this Figure, a true bare table impedance measurement is compared to one made with the mounting hole blocked with (nearly massless) plastic tape. The profound increase in “Q” that results from having the mounting hole open clearly reflects into the imped-



Figure 11. Experimental arrangement used to illustrate force/motion/voltage/current relationships. The current driving the shaker is monitored by a clamp-on instrument-grade current transformer. An ICP impedance-head measures the force delivered by the shaker and the motion of its table. A 76.97 gram stainless-steel cylinder is fitted as a test mass.

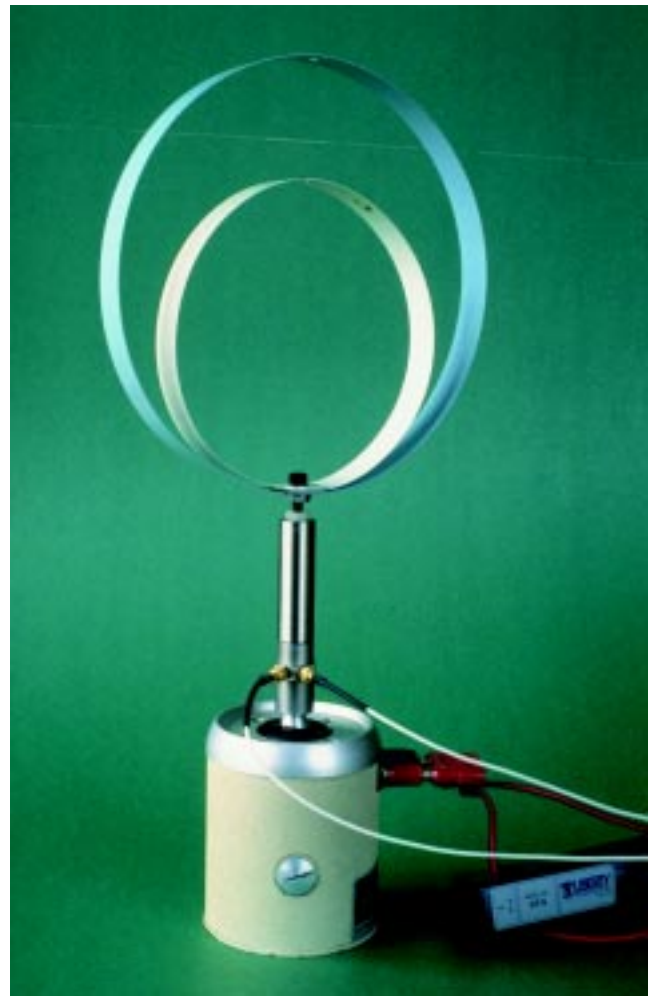


Figure 12. Dual-ring structure used to simulate “high Q” response in a driven shaker load. This structure exhibits several lightly damped modes in the frequency range studied.

ance. When taped over, the impedance rises to a little less than 5  $\Omega$  at resonance; when this hole is open, the impedance soars to nearly 15  $\Omega$ .

### Deeper Reflections

The shaker and the article it tests become a closely coupled system; each influences the other. Figures 11 and 12 show the mechanical configurations of two table-mounted shake tests, one driving a rigid mass, the other with a structure exhibiting

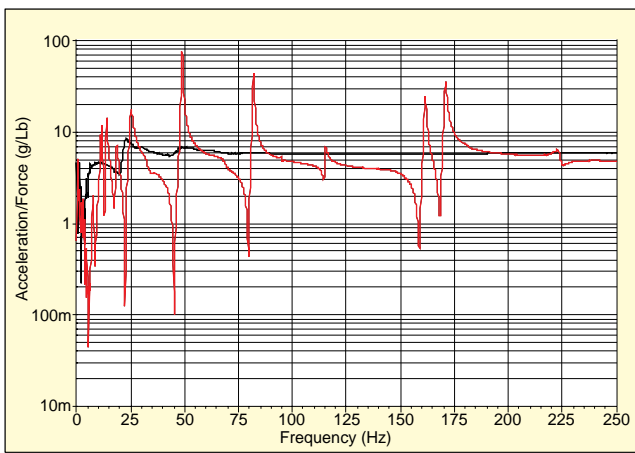


Figure 13. Inertance of two test loads subjected to random testing. The black trace resulted from shaking the cylindrical mass shown in Figure 11. The dynamically active red trace illustrates the effect of attaching the dual-ring structure to the cylinder as shown in Figure 12.

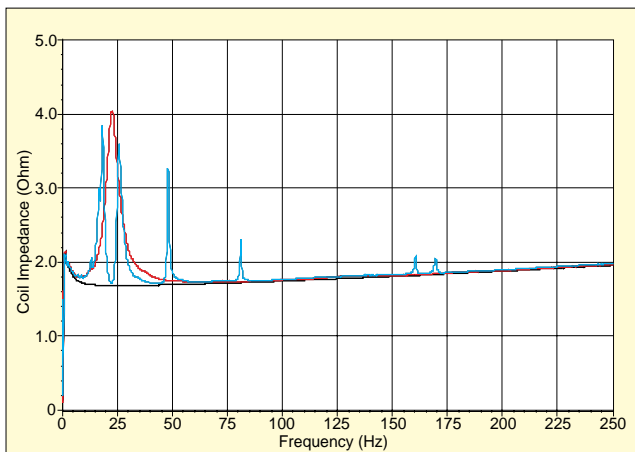


Figure 14. Coil impedance reflected by the dual-rings (blue) and its base mass only (red). For reference, the "blocked table" results are repeated (black). Note that the dynamics of the load invariably lead to an increase in the coil impedance, never a reduction. The minimum impedance is that RL behavior exhibited in the blocked test.

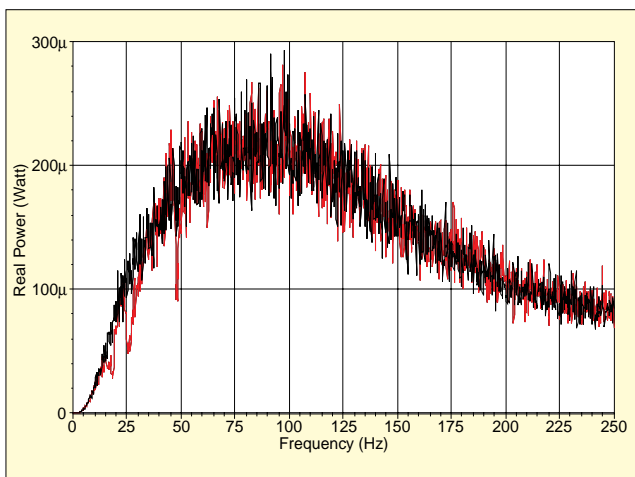


Figure 15. Real Power dissipated by the shaker while driving the structure of Figure 12 (red) compared to that of a "blocked table" test (black). Note that high-Q resonances produce a slight reduction in power required over their bandwidth.

considerable compliance within the frequency range of testing.

Figure 13 compares the acceleration/force frequency response functions that resulted from testing these structures. In an ideal world, the rigid mass test (black trace) would yield a constant value equal to the reciprocal of the cylinder's 76.97 gram (0.1693 lb/g) mass. In this experiment, these characteristics are true above about 50 Hz. The slight undulations in this

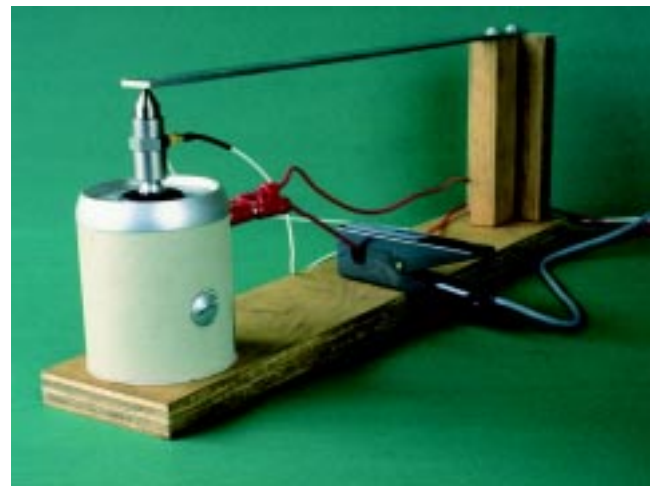


Figure 16. Mechanical arrangement used to implement a "ground referenced" shaker examination rather than the "free-free" arrangement of Figures 11 and 12. Here, a small conical titanium tip is used to drive a cantilever beam; this arrangement eliminates concerns about imposing rotational moments at the drive site.

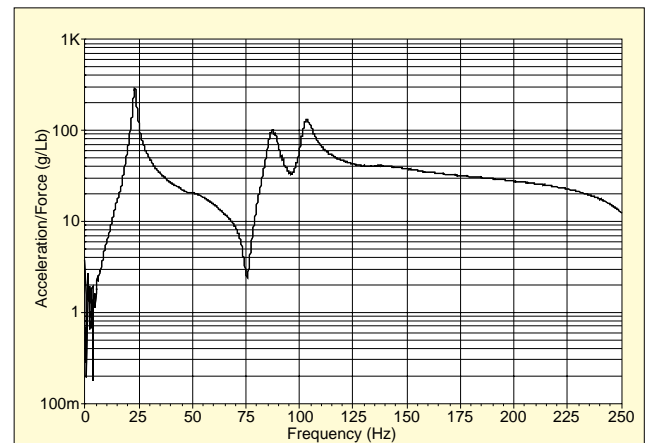


Figure 17. Inertance of tip-driven cantilever beam. Note, in contrast to Figure 13, that the first singularity encountered is a resonance, not an antiresonance. This is characteristic of any constrained (rather than free-free) shake.

trace at low frequency could probably be traced to unintended "rocking" motions of the specimen at low frequencies, caused in part by the high CG location and slight inertial dissymmetries due by the impedance-head connectors and cables. Resulting moments likely introduced some base-strain response in the driving-point sensor.

This same cylinder is the bulk of the more compliant structure's mass (by intention). The blue trace from the dual-ring test is clearly centered about the result from the cylinder-alone trace as expected. Note that these are both true free-free shakes with regard to the excitation degree of freedom; no external springs support or restrain the test item. All static support comes from the "upstream" side of the driving-point transducer. In aircraft modal testing parlance, these are "ignorable-coordinate" shakes. Because these tests are of free-free form, the lowest frequency singularity encountered is an *antiresonance* (a local minimum) as theory predicts. The rigid body translational mode is truly at zero frequency, not merely at a low frequency as found in a spring-supported approximation of free-free conditions.

Figure 14 presents the impedance of the shaker coil during the mass test (red) and dual-ring test (blue). For reference, the blocked impedance is repeated. Note that the impedance in both of these tests show local maxima around each resonance of the test article. The lowest frequency spike in this Figure is determined by the shaker stiffness and the mass of the structure added to the shaker's moving mass. Clearly, the "baseline" of the impedance during either test is the blocked value. Reso-

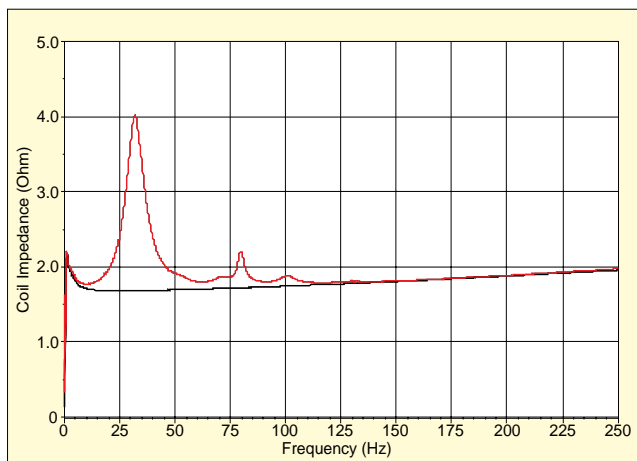


Figure 18. Shaker coil impedance exhibited while driving a cantilever beam (blocked table in black).

nant activity increases the impedance, it never lowers it below the blocked value. Hence the blocked impedance provides the conservative (worst case) estimate of amplifier power required for any test at any frequency.

This point is further made by Figure 15 which compares the measured real power dissipated by the shaker during the dual-ring test (red trace) to that consumed during a blocked armature test (black trace) with the same random input applied to the power amplifier. These traces were computed as the real component of the cross-spectrum between shaker input terminal voltage and shaker drive current. Note that the only significant difference between these very different test conditions is a slight reduction in dissipated power at the structure's resonances.

Figure 16 shows the hardware configuration of a very different type of shake test, one termed a "constrained-structure," "statically determinant" or "ground-referenced" shake. The structure is said to be constrained and therefore statically determinant because it has attachment to earth through sufficient degrees-of-freedom to maintain it in position. In contrast, our prior test excited one degree-of-freedom (an "ignorable coordinate") that would need to be grounded to render the structure statically determinant.

Here a simple cantilever beam is excited near its tip using a shaker and impedance-head. As a matter of craft, the connecting drive is a conical tip pressed against the structure and held in pre-load against it by the shaker's suspension. This driving arrangement prevents applying unwanted (and unmeasured) moments to the test article. This benefit is gained at the cost of available shaker stroke. For most constrained modal studies this is an attractive trade, particularly if more than one drive-site will be used *in sequence*.

Figure 17 illustrates the acceleration/force frequency response function measured from the cantilever's tip. Note that the lowest frequency singularity in this shake is a *resonance* as theory and common understanding would suggest. This affirms that all of this structure's rigid-body modes are at non-zero frequency, owing to its sufficient boundary constraints to ground. As this measurement is a driving-point observation, it exhibits an alternation of resonant maxima and antiresonant minima as does the free-free shake of Figure 13.

Figure 18 presents the corresponding coil impedance. Again, the coil impedance rises near each resonance and exhibits a "floor" equal to the "blocked armature" measurement of Figure 9. Since the shaker table is obliged to move only with the dynamic freedom of the beam, there is no peak at a frequency determined by the total mass of the structure (plus shaker moving mass) and the stiffness of the shaker suspension as there is in Figure 14.

## Taking Control of the Situation

The foregoing observations prepare us to appreciate the per-

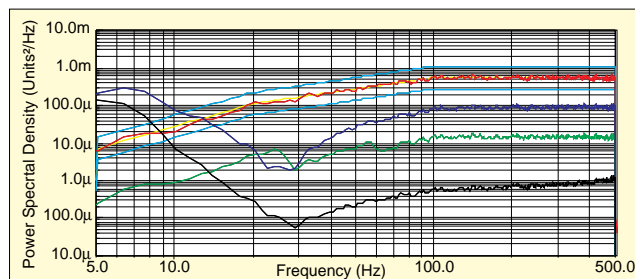


Figure 19. Various signals resulting while shaking the mass load of Figure 11 in a closed-loop random test. In this examination, a shaped test profile of 0.5 g (rms) was applied. The profile follows a constant displacement line from 5 to 20 Hz, constant velocity from 20 to 100 Hz and constant acceleration from 100 to 500 Hz. The power spectral densities of acceleration (red), force (green), shaker current (purple) and amplifier input voltage (black) are shown.

formance of the shaker when applied in a control loop. Our initial interest focuses upon the rigid mass payload shake-test configuration of Figure 11. Performance under several random tests is considered.

In Figure 19, a controlled acceleration shake is presented. In this test, a servo-loop was formed using the impedance head's acceleration output as the feedback signal. The power amplifier was driven with a signal continuously modified by the servo-loop to maintain the acceleration equal to an input command profile. That profile is the yellow line traced by the red acceleration line and bounded by parallel  $\pm 3$  dB limit lines (light blue) in Figure 19.

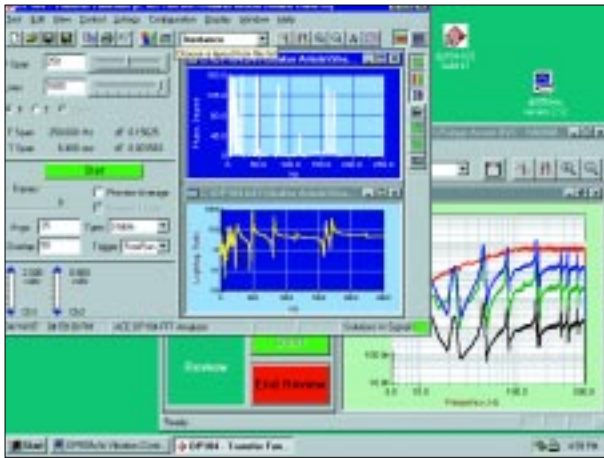
The selected profile was an arbitrary choice. The servo-controller was programmed to test over a 5 to 500 Hz frequency span with three distinct regions. A constant acceleration PSD ( $g^2/Hz$ ) was specified between 100 and 500 Hz. In the 20 to 100 Hz region the target is a constant velocity power spectral density or an acceleration PSD that increases in proportion to frequency. In the 5 to 20 Hz region the target shifts to a constant displacement PSD, an acceleration spectrum that increases in proportion to frequency squared. The overall amplitude of this response was specified to be 0.5 g (rms).

Power Spectral Density profiles may be unfamiliar to some readers. A (loosely) corresponding swept-sine test might prescribe a composite sweep composed of constant 2.5 mil (rms) displacement from 5 to 20 Hz, constant 0.31 in./sec (rms) velocity from 20 to 100 Hz and constant 0.5 g (rms) acceleration of from 100 to 500 Hz. Expressed as an acceleration sweep profile this equates to 0.00625 g (rms) at 5 Hz increasing in proportion to frequency squared to 0.1 g (rms) at 20 Hz, then increasing in proportion to frequency to 0.5 g (rms) at 100 Hz, then remaining constant at 0.5 g (rms) to 500 Hz. With this sweep profile, the rms g value would increase rapidly between 5 and 20 Hz, less rapidly from 20 to 100 Hz and then remain constant at 1 g to 500 Hz.

The behavior of a random test is different. The excitation does not focus on a single frequency at any instant in time. Instead, it excites all frequencies, simultaneously with random fluctuation in amplitude and phase at every frequency. On average, the prescribed spectral shape is maintained. The rms value of the signal constantly targets 0.5 g regardless of the specific frequency content; again, this characteristic is maintained on average. Hence the spectral profile shown by the yellow line in Figure 19 is a statistical target. The area under this curve is the prescribed signal's *mean square value*, the square root of this integral is the target rms signal value.

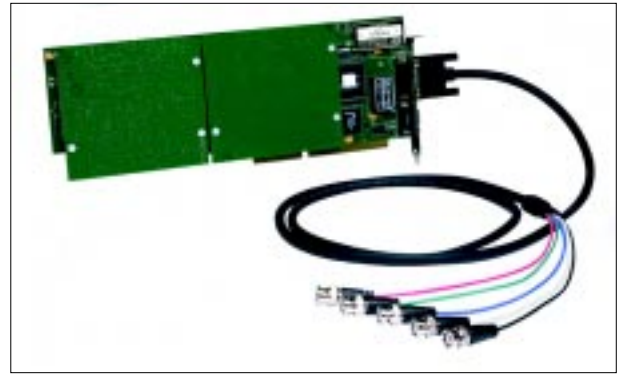
Figure 19 illustrates that the shaker can be controlled to follow the required random profile through all three regions, constant displacement, velocity and acceleration based upon the acceleration (red) feedback signal. It also shows the required (averaged) variations by frequency of the driving force, current and shaker input voltage to accomplish this. In this test, the payload is a nonresonant mass. Note the flat spectral shape of the force (green) and current (purple) signals in the constant acceleration region from 100 to 500 Hz. Since the driven load

## Data Physics Instruments Used in this Article



Two new Data Physics products were used in the preparation of this article, the DP104 ACE FFT Analyzer and the DP550Win Vibration Controller. Both provide 32-bit Windows 95 (and NT) compatible software, reflecting the highest standards of compliance with Microsoft's operating systems. These products use different signal processing hardware and focus upon different application areas, yet they exhibit a common operational "look and feel." ACE and DP550Win function synergistically; they can run *concurrently* in the same computer, facilitating sophisticated analysis of shake-test data or a broad range of other phenomena. These products integrate seamlessly with other Windows applications running on your PC and its accessories.

The DP550Win is a third-generation hardware/software product family incorporating field-proven modular ISA hardware, industry-standard algorithm modules and the most modern control/analysis interface in the field. This system can control swept-sine, random, classical shock, arbitrary transient, sine-on-random and random-on-random tests. Configurations from 3 to 16 inputs are offered. Patented processes provide the most rapid loop-control time-constant offered by any manufacturer. Sophisticated options such as Shock Response Spectrum (SRS) control permit testing to the most demanding specifications. The human interface makes such tasks straightforward, reflecting over a



decade's experience at the forefront of this technology.

The ACE DP104 FFT is the world's smallest FFT analyzer, yet one of the most powerful. ACE is a two channel analyzer packaged in a type III PCMCIA card. This tiny (1.8 oz) device provides two 16-bit inputs, two independent 16-bit signal sources and a 50 MHz 32-bit floating-point DSP. It hides in the PC-card slot of a laptop or in an inexpensive desktop card reader. ACE provides 100 dB dynamic range, variable transforms from 64 to 4096 point and a 20 kHz real-time bandwidth. Options include real-time Zoom, extended transforms to 65,536 points (25,600 spectral lines), waterfall and spectrogram capture and 20 kHz real-time disk recording/playback/analysis.



is simply a mass,  $F = Ma$  applies and the force required to produce constant acceleration is also a constant. Since the shaker produces a force in proportion to current, the drive current required is also a constant in this region. This proportionality does not exist anywhere outside of the 100 to 500 Hz constant acceleration range.

Figure 20 reinforces the concept of proportionality within the 100 to 500 Hz band. Here, the servo-loop has been reconfigured to control the force, not the acceleration. The same target spectral *shape* has been used, but the target rms value has been scaled by the driven mass (76.97 gram or 0.1693 lb/g) to 0.0845 lb (rms). Note that essentially the same acceleration is exhibited within the 100 to 500 Hz range. Also note the change in all signals outside of this frequency span.

In Figure 21, the test is repeated again with the servo-loop closed around the current provided to the shaker. The test profile shape remains the same; the rms target is changed to 0.2008 amperes (rms) based upon the ratio of force/current ratio ( $k_2 = 0.4208 \text{ lb/A}$ ) measured from Figure 19. Again, the proportionality is validated within the constant acceleration region of this driven mass test. Note the similar acceleration PSD level between 100 and 500 Hz in Figures 19, 20 and 21.

Were life so simple that all shake tests were performed on rigid masses, shaker control systems would not be required

stock-in-trade facilities. We could simply use a transconductance amplifier (one that provides a current output proportional to its voltage input) to drive the shaker. This would result in an acceleration proportional to the input command voltage. Note that a common (voltage-output) power amplifier could never accomplish this owing to the inductive impedance component of the shaker's voice coil; such an amplifier tends to produce jerk ( $d^3x/dt^3$ ) proportional to input voltage when driving a pure-mass payload.

But life is not that simple and if we must excite real structures to specified profiles, servo-control is the only practical means of achieving this. This point is substantiated by Figures 22 and 23 that present the acceleration, force, current and voltage signals associated with the application of the acceleration profile of Figure 19 to two different structures with resonant behavior within the test bandwidth.

In Figure 22, the dual-ring structure of Figure 12 is subjected to our three zone profile under table-acceleration control. Note that the servo-loop has no difficulty in achieving this, but that none of the other signals bear any proportional relationship to the acceleration in any frequency range; this is simply not an " $F = Ma$ " situation! The same observation can be made of Figure 23 which presents the results of testing the cantilever beam structure of Figure 16. SV

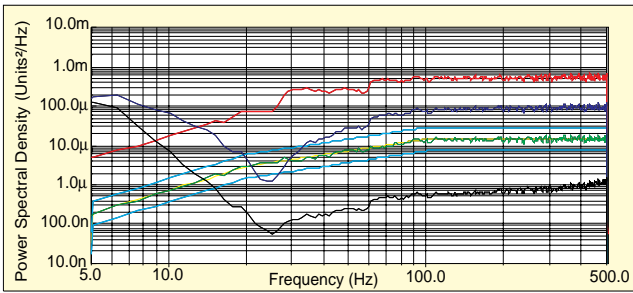


Figure 20. Repeat of the test shown in Figure 19 with the servo loop closed around the force measurement. The test profile retained the same shape but was scaled (by the test mass) to 0.0845 lb (rms). Compare with Figure 19 and note the similar results in the 100 to 500 Hz range of "constant acceleration."

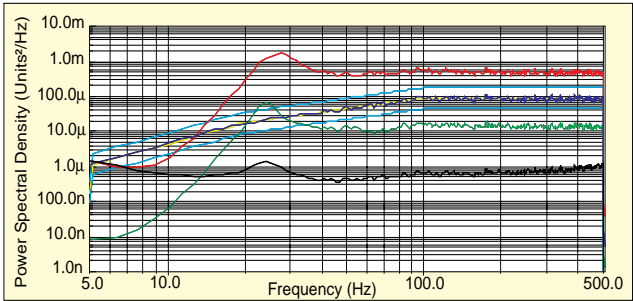


Figure 21. Another repeat of the prior test with the control loop closed around the current driving the shaker. The target spectral shape remains the same but is scaled by the current/ acceleration ratio of Figure 19 to 0.2008 amperes (rms). Compare with Figures 19 and 20, noting the similar performance in the "constant force and acceleration" region between 100 and 500 Hz.

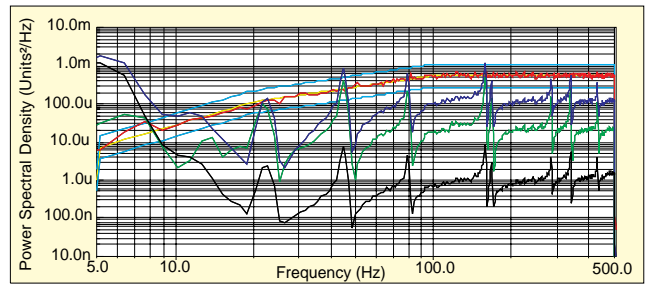


Figure 22. Controlled acceleration test to the same profile as Figure 19 applied to the dual ring structure of Figure 12. Note that force or current control could not produce similar response results in any portion of this spectrum ( $F \neq Ma!$ ).

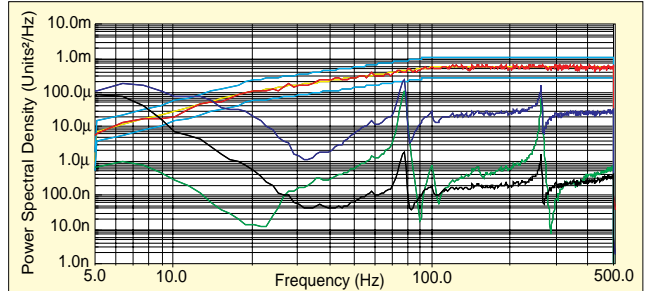


Figure 23. The same controlled acceleration test performed upon the constrained beam of Figure 16. Note, again, that force or current control could not produce the same responses. Note further, from Figures 19 through 23, that an "open loop" voltage signal will not produce a constant force, acceleration, velocity or displacement result; to the first approximation, it will produce "constant jerk" owing to its coil inductance.